

# DisDiff: Unsupervised Disentanglement of Diffusion Probabilistic Models

Tao Yang<sup>1</sup> Yuwang Wang<sup>2</sup> Yan Lv<sup>3</sup> Nanning Zheng<sup>1</sup>

## Abstract

In this paper, targeting to understand the underlying explainable factors behind observations and modeling the conditional generation process on these factors, we propose a new task, disentanglement of diffusion probabilistic models (DPMs), to take advantage of the remarkable modeling ability of DPMs. To tackle this task, we further devise an unsupervised approach named DisDiff. For the first time, we achieve disentangled representation learning in the framework of diffusion probabilistic models. Given a pre-trained DPM, DisDiff can automatically discover the inherent factors behind the image data and disentangle the gradient fields of DPM into sub-gradient fields, each conditioned on the representation of each discovered factor. We propose a novel Disentangling Loss for DisDiff to facilitate the disentanglement of the representation and sub-gradients. The extensive experiments on synthetic and real-world datasets demonstrate the effectiveness of DisDiff.

## 1. Introduction

As one of the most successful generative models, diffusion probabilistic models (DPMs) achieves remarkable performance in image synthesis. They use a series of probabilistic distributions to corrupt images in the forward process and train a sequence of probabilistic models converging to image distribution to reverse the forward process. Despite the remarkable success of DPM in tasks such as image generation (Song et al., 2020b), text to images (Saharia et al., 2022), image editing (Meng et al., 2021), little attention has been paid on the representation learning (Zhang et al., 2022) based on DPM. Diff-AE (Preechakul et al., 2022) and PADE (Zhang et al., 2022) are the two methods proposed recently for representation learning by reconstructing the images in the DPM framework. However, the learned la-

tent representation can only be interpreted relying on an extra pre-trained with predefined semantics linear classifier. Although there are some degrees of freedom during implementation, in this paper, we will refer DPMs exclusively to the Denoising Diffusion Probabilistic Models (DDPMs) (Ho et al., 2020).

On the other hand, disentangled representation learning (Higgins et al., 2018) aims to learn the representation of the underlying explainable factors behind the observed data and is thought to be one of the possible ways for AI to understand the world fundamentally. Different factors correspond to different kinds of image variations, respectively, and independently. Most of the methods learn the disentangled representation based on generative models, such as VAE (Higgins et al., 2017; Chen et al., 2018; Kim & Mnih, 2018) and GAN (Lin et al., 2020). The VAE-based methods have an inherent trade-off between the disentangling ability and generating quality (Higgins et al., 2017; Chen et al., 2018; Kim & Mnih, 2018). The GAN-based methods suffer from the problem of reconstruction due to the difficulty of gan-inversion (Wang et al., 2022). To the best of our knowledge, there is no method of learning disentangled representation using DPM.

In this paper, we connect DPM to disentangled representation learning, for the first time, and propose a new task: the disentanglement of DPM. Given a pre-trained DPM model, the goal of disentanglement of DPM is to learn disentangled representations for the underlying factors in an unsupervised manner, and learn the corresponding disentangled conditional sub-gradient fields, with each conditioned on the representation of each discovered factor.

The benefits of the disentanglement of DPM are two-folds: (i) It enables totally unsupervised controlling of images by automatically discovering the inherent semantic factors behind the image data. These factors helps to extends the DPM conditions information from human defined ones such as annotations (Zhang et al., 2022)/image-text pairs (Kawar et al., 2022), or supervised pre-trained models (Kim et al., 2022) such as CLIP (Radford et al., 2021). One can also flexibly sample partial conditions on the part of the information introduced by the superposition of the sub-gradient field, which is novel in existing DPM works. (ii) DPM has remarkable performance on image generation quality,

<sup>1</sup>Xi'an Jiaotong University <sup>2</sup>Tsinghua University

<sup>3</sup>Microsoft Research Asia. Contact Tao Yang by <yt14212@stu.xjtu.edu.cn>. Correspondence to: Yuwang Wang <wang-yuwang@mail.tsinghua.edu.cn>.

and is naturally friendly for the inverse problem, e.g., the inversion of DDIM (Song et al., 2020a), PADE. Compared to VAE (trade-off between the disentangling ability and generating quality) or GAN (problem of gan-inversion), DPM is a better framework for disentangled representation learning. Besides, as Locatello et al. (2019) points out, other inductive biases should be proposed except for total correlation. DPM makes it possible to adopt constraints from all different timesteps as a new type of inductive bias. Further, as Srivastava et al. (2020) points out, the information of data includes: factorized and non-factorized. DPM has the ability to sample non-factorized (non-conditioned) information (Ho & Salimans, 2022), which is naturally fitting for disentanglement.

To address the task of disentangling the DPM, we further propose a unsupervised solution for the disentanglement of a pretrained DPM, named as DisDiff. DisDiff adopts an encoder to learn the disentangled presentation for each factor, and a decoder to learn the corresponding disentangled conditional sub-gradient fields. We further propose a novel Disentangling Loss to make the encoded representation satisfy the disentanglement requirement, and reconstruct the input image as well.

Our main contributions can be summarized as follows:

- We present a new task: disentanglement of DPM, disentangling a DPM into several disentangled sub-gradient fields, which can improve the interpretability of DPM.
- We build an unsupervised framework for disentanglement of DPM, DisDiff, which not only learns a disentangled representation but also disentangled gradient field for each factor.
- We propose a Disentangling Loss for DPM to facilitate the disentanglement of different factor conditions and the sub-gradient fields.

## 2. Related Works

**Diffusion Probabilistic Models** DPMs have achieved comparable or superior image generation quality (Sohl-Dickstein et al., 2015; Song & Ermon, 2019; Ho et al., 2020; Song et al., 2020b; Jolicœur-Martineau et al., 2020) than GAN (Goodfellow et al., 2020). Diffusion-based image editing has drawn much attention, and there are mainly two categories of works. Firstly, image-guided works edit an image by mixing the latent variables of DPM and the input image (Choi et al., 2021; Lugmayr et al., 2022; Meng et al., 2021). However, using images to specify the attributes for editing may cause ambiguity, as pointed out by Kwon et al. (2022). Secondly, the classifier-guided works (Dhariwal & Nichol, 2021; Avrahami et al., 2022; Liu et al., 2023)

edit image by utilizing the gradient of an extra classifier. These methods require calculating the gradient, which is costly. Meanwhile, these methods require annotations or models pre-trained with labeled data. In this paper, we propose DisDiff to edit the image in an unsupervised way. On the other hand, little attention has been paid to representation learning in the literature on the diffusion model. Two related works are Diff-ae (Preechakul et al., 2022) and PADE (Zhang et al., 2022). Diff-ae (Preechakul et al., 2022) proposes a diffusion-based auto-encoder for image reconstruction. PADE (Zhang et al., 2022) uses a pre-trained DPM to build an auto-encoder for image reconstruction. However, the latent representation learned by these two works does not explicitly respond to the underlying factors of the dataset. To the best of our knowledge, our DisDiff is the first diffusion-based framework for disentangled representation learning.

**Disentangled Representation Learning** Bengio et al. (2013) introduced disentangled representation learning. The target of disentangled representation learning is to discover the underline explanatory factors of the observed data. The disentangled representation is defined as each dimension of the disentangled representation corresponding to an independent factor. Based on such a definition, some VAE-based works achieve disentanglement (Chen et al., 2018; Kim & Mnih, 2018; Higgins et al., 2017; Burgess et al., 2018) only by the constraints on probabilistic distributions of representations. Locatello et al. (2019) points out the identifiable problem by proving that only these constraints are not enough for disentanglement, and extra inductive bias is required. For example, Yang et al. (2021) proposes to use symmetry properties modeled by group theory as inductive bias. Most of the methods of disentanglement are based on VAE. There are also some works based on GAN, including leveraging pretrained generative model (Ren et al., 2021). Our DisDiff introduces the constraint of all time steps during the diffusion process as a new type of inductive bias. Furthermore, DPM is capable of sampling non-factorized (non-conditioned) information (Ho & Salimans, 2022), which is naturally fitting for disentanglement. In this way, we shed light on disentanglement based on a new framework of the DPM.

## 3. Background

### 3.1. Diffusion Probabilistic Models (DPM)

We take DDPM (Ho et al., 2020) as an example. DDPM adopts a sequence of fixed variance distributions  $q(x_t|x_{t-1})$  as the forward process to collapse the image distribution  $p(x_0)$  to  $\mathcal{N}(0, I)$ . These distributions are

$$q(x_t|x_{t-1}) = \mathcal{N}(x_t; \sqrt{1 - \beta_t}x_{t-1}, \beta_t I). \quad (1)$$

Then we can sample  $x_t$  by the following formula  $x_t \sim \mathcal{N}(x_t; \sqrt{\alpha_t}x_0, (1 - \bar{\alpha}_t))$ , where  $\alpha_t = 1 - \beta_t$  and  $\bar{\alpha}_t = \prod_{i=1}^t \alpha_i$ , i.e.,  $x_t = \sqrt{\alpha_t}x_0 + \sqrt{1 - \bar{\alpha}_t}\epsilon$ . The reverse process is fitting by other distributions parameterized by  $\theta$ :

$$p_\theta(x_{t-1}|x_t) = \mathcal{N}(x_t; \mu_\theta(x_t, t), \sigma_t I). \quad (2)$$

where  $\mu_\theta(x_t, t)$  is parameterized by a Unet  $\epsilon_\theta(x_t, t)$ . The training of it is to minimize the variational upper bound of negative log-likelihood:

$$\mathcal{L}_\theta = \mathbb{E}_{x_0, t, \epsilon} \|\epsilon - \epsilon_\theta(x_t, t)\|. \quad (3)$$

### 3.2. Representation learning from DPMs

The classifier-guided method (Dhariwal & Nichol, 2021) uses the gradient of pre-trained classifier  $\nabla_{x_t} \log p(y|x_t)$  to impose a condition on pre-trained DPM and obtain a new conditional DPM:  $\mathcal{N}(x_t; \mu_\theta(x_t, t) + \sigma_t \nabla_{x_t} \log p(y|x_t), \sigma_t)$ . Based on the classifier-guided sampling method, PADE (Zhang et al., 2022) proposes a method to learn auto-encoder for pre-trained DPM. Specifically, given a pre-trained DPM, PADE introduces an encoder  $E_\phi$ , and the representation can be derived by  $z = E_\phi(x_0)$ . They use a gradient estimator  $G_\psi(x_t, z, t)$  to simulate gradient  $\nabla_{x_t} \log p(z|x_t)$  for reconstruction.

By this means, they use it to assemble the unconditional DPM as a new conditional DPM as the decoder. Similar to regular DPM  $\mathcal{N}(x_t; \mu_\theta(x_t, t) + \sigma_t G_\psi(x_t, z, t), \sigma_t)$ , we can use the following objective to train encoder  $E_\phi$  and the network  $G_\psi$ :

$$\mathcal{L}_\psi = \mathbb{E}_{x_0, t, \epsilon} \|\epsilon - \epsilon_\theta(x_t, t) + \frac{\sqrt{\alpha_t} \sqrt{1 - \bar{\alpha}_t}}{\beta_t} \sigma_t G_\psi(x_t, z, t)\|. \quad (4)$$

## 4. Method

In this section, we first introduce the formulation of the proposed task in Section 4.1. Then we present the overview of DisDiff in Section 4.2. After that, we present the detailed implementation of the proposed Disentangling Loss in Section 4.3 and how to balance it with reconstruction loss in Section 4.4. Finally, in Section 4.5, we discuss the relation between Disentangling Loss and the total correlation, which is a necessary condition for disentanglement.

### 4.1. Disentanglement of DPM

We assume that dataset  $\mathcal{D}$  is generated by  $N$  underlying ground truth factors  $N$  factors  $\mathcal{C} = \{1, 2, \dots, N\}$ . For example, for Shapes3D, the underlying concept factors include background color, floor color, object color, object shape, object scale, and pose. Therefore, there is a one-one mapping

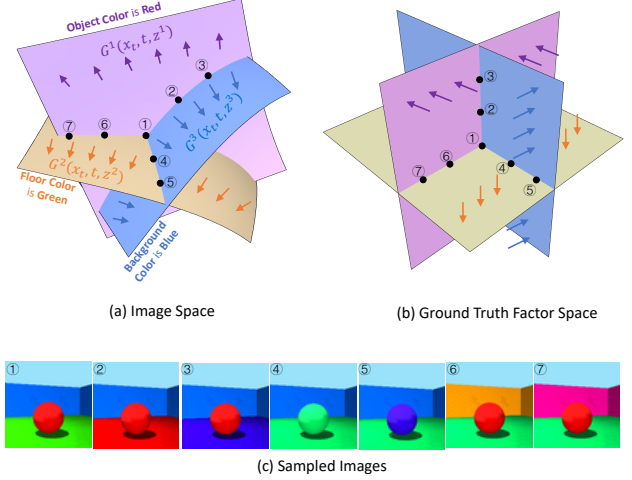


Figure 1. Illustration of disentanglement of DPMs. (a) is the diagram of image space. (b) is the diagram of factor space. (c) is the demonstration of sampled images. Surface indicates the conditional distribution of a single factor  $p(x|z^c)$ . Different colors correspond to different factors. Here we show three factors: object color, background color, and floor color. Arrows are gradient fields  $\nabla_{x_t} \log p(z^c|x_t)$  parameterized by  $G_\phi^c(x_t, t, z^c)$ . The learned  $G_\phi^c(x_t, t, z^c)$  converges the noise data to the conditional distribution. The black points are the sampled images, which are shown in (c).

between each sample and each tuple of factor representations,  $h : x_0 \mapsto (f^1, \dots, f^N), \forall x_0 \in \mathcal{D}$ . The data distribution  $p(x)$  can be disentangled into  $N$  independent distributions  $\{p(x|f^k) | k = 1, \dots, N\}$ , and each conditioned on only one factor, which is shown as the curved surface of image space in Figure 1(a). The DPM learns a sequence of distributions  $\{p_t(x) | t = T, T-1, \dots, 0\}$  converging to  $p(x)$ . Such convergence is achieved by optimizing the corresponding gradient fields  $\{\nabla_x \log p_t(x) | t = T, T-1, \dots, 0\}$  (learned by  $\epsilon_\theta$  with parameters  $\theta$ ). The disentangled DPM contains  $N$  sequences of distributions, converging to  $N$  distributions  $\{p(x|f^c) | c = 1, \dots, N\}$  respectively. The target of disentanglement of a DPM is, for each factor  $c$ , to learn  $G_\psi^c$  to estimate  $\nabla_x \log p_t(x|f^c)$ , which corresponds to the arrows pointing to the curve surface in Figure 1(a). One may note that in the data sample space, such as image space, the curved surfaces indicate that the data sample space is not well-organized, and the variations of the factors are entangled. Compared to the image space, the ground truth factor space is well-organized, and the subspaces of factors are orthogonal between each other, as shown in Figure 1(b). Disentangled representation learning aims to model the ground truth factor space using an encoder  $E_\phi$ , which encodes the raw data into disentangled representations. The disentangled representation is ideal for representing the conditions for the conditional distributions  $\{p(x|f^c) | c = 1, \dots, N\}$  of the disentangled DPM. Conditioned on the disentangled

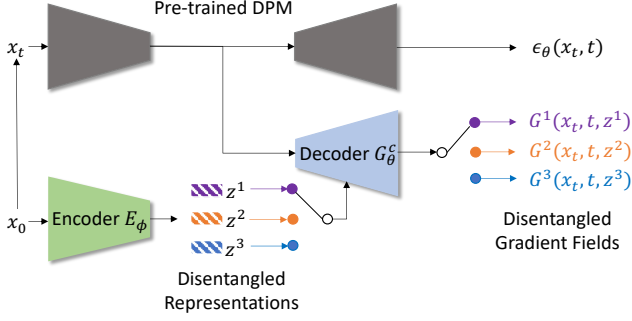


Figure 2. Illustration of DisDiff. Gray networks indicate the pre-trained Unet of DPM  $\epsilon_\theta(x_t, t)$ . Image  $x_0$  is first to be encoded to representations  $\{z^1, z^2, \dots, z^N\}$  of different factors by encoder  $E_\phi$  ( $N = 3$  in the figure). We thus decode the representations by decoder  $G_\theta^c$ . By this means, we can obtain the gradient field of the corresponding factor. With the obtained gradient field, we can sample the image under the corresponding condition.

representation, the disintangled DPM can flexibly generate the data samples. In this paper, we propose a method named DisDiff, as a solution for the disentanglement of a DPM.

#### 4.2. Overview of DisDiff

The overview framework of DisDiff is shown in Figure 2. Given a pre-trained unconditional DPM on dataset  $\mathcal{D}$  with  $N$  factors  $\mathcal{C} = \{1, 2, \dots, N\}$ , e.g., a DDPM model with parameters  $\theta$ ,  $p_\theta(x_{t-1}|x_t) = \mathcal{N}(x_{t-1}; \mu_\theta(x_t, t), \sigma_t)$ , our target is to disentangle the DPM in an unsupervised manner. Specifically, given  $x_0 \in \mathcal{D}$ , for each factor  $c \in \mathcal{C}$ , the goal is to learn the disintangled representation  $z^c$  via an encoder  $E_\phi$  (with learnable parameters  $\phi$ ) as  $E_\phi(x_0) = \{E_\phi^1(x_0), E_\phi^2(x_0), \dots, E_\phi^N(x_0)\} = \{z^1, z^2, \dots, z^N\}$ , and the disintangled gradient field  $\nabla_{x_t} \log p(z^c|x_t)$ . Therefore, the conditional reverse process (condition on factors  $\mathcal{S} \subseteq \mathcal{C}$ , and  $z^{\mathcal{S}} = \{z^c|c \in \mathcal{S}\}$ ) can be formulated by a Gaussian distribution  $p_\theta(x_{t-1}|x_t, z^{\mathcal{S}})$  with a shifted mean:

$$\mathcal{N}(x_{t-1}; \mu_\theta(x_t, t) + \sum_{c \in \mathcal{S}} \nabla_{x_t} \log p(z^c|x_t), \sigma_t). \quad (5)$$

Since  $p(z^c|x_t)$  is intractable, we use  $G_\psi^c(x_t, z^c, t)$ ,  $c \in \mathcal{C}$ , with learnable parameters  $\psi$ , to estimate the gradient fields  $\nabla_{x_t} \log p(z^c|x_t)$ ,  $c \in \mathcal{C}$ .

With different options of  $\mathcal{S}$ , one can flexibly devise the approximator following score-based conditioning trick (Song et al., 2020b; Song & Ermon, 2019) as follows:

$$\epsilon_\psi(x_t, z^{\mathcal{S}}, t) = \epsilon_\theta(x_t, t) - \sum_{c \in \mathcal{S}} \sqrt{1 - \bar{\alpha}_t} G_\psi^c(x_t, z^c, t). \quad (6)$$

Then one can derive the corresponding data sample using Tweedie’s Formula as:

$$\hat{x}_0^{\mathcal{S}} = \frac{x_t - \sqrt{1 - \bar{\alpha}_t} \epsilon_\psi(x_t, z^{\mathcal{S}}, t)}{\sqrt{\bar{\alpha}_t}}. \quad (7)$$

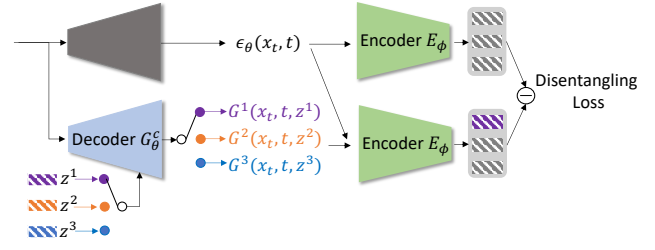


Figure 3. The demonstration of disentangling loss. We first sample a factor  $c$  and then decode the representation  $z^c$  to obtain the gradient field of the corresponding factor. With this gradient field, we can obtain the predicted  $x_0$  of the corresponding factor. On the other hand, we can obtain predicted  $\hat{x}_0$  of the original pre-trained DPM. We then encode the images into two different representations and calculate the disentangling loss.

For example, one can choose only one disintangled factor, i.e., setting  $\mathcal{S} = c$ , and use the gradient  $\nabla_{x_t} \log p(z^c|x_t)$  (only conditioned on  $z^c$ ) to guide the sampling of the pre-trained DPM, resulting in the predicted sample  $\hat{x}_0^c$ . We leave  $\hat{x}_0$  to denote the predicted data sample using the pretrained unconditioned DPM  $\epsilon_\theta(x_t, t)$ .

According to the *completeness* requirement of disentanglement, the disintangled representation  $E_\phi(x_0)$  should contain the full information of sample  $x_0$ , i.e., one can reconstruct  $x_0$  by using all the disintangled representations  $E_\phi(x_0)$  as a condition. Following Equation 7, we set  $\mathcal{S} = \mathcal{C}$  to include all the disintangled representation, resulting in the derived data sample  $\hat{x}_0^{\mathcal{C}}$ . One may note that this is exactly the reconstruction case in PDAE. Here, we adopt the same reconstruction loss, denoted as

$$\mathcal{L}_r = \mathbb{E}_{x_0, t, \epsilon} \|\epsilon - \epsilon_\theta(x_t, t) + \frac{\sqrt{\alpha_t} \sqrt{1 - \bar{\alpha}_t}}{\beta_t} \sigma_t \sum_{c \in \mathcal{C}} G_\psi^c(x_t, z^c, t)\|. \quad (8)$$

Besides the above *completeness* requirement, each disintangled representation should only reflect one corresponding factor independently, i.e., the *disentanglement* requirement. We devise a novel loss, named Disentangling Loss, to achieve the disentanglement of the pre-trained DPM. In the following, we will present the Disentangling Loss and the total loss.

#### 4.3. Disentangling Loss

In this section, we provide the detailed implementation of Disentangling Loss. As discussed above, given sample  $x_0$  and its disintangled representation  $E_\phi(x_0)$ , we randomly sample  $c \in \mathcal{C}$  and use  $\mathcal{S} = c$  to get the conditioned sample  $\hat{x}_0^c$  (only conditioned on representation  $z^c$ ). According to the disentanglement requirement, compared to the unconditioned predicted image  $\hat{x}_0$  (sampling with the pre-trained unconditioned DPM  $\epsilon_\theta(x_t, t)$ ),  $\hat{x}_0^c$  should satisfy the



following two conditions: (i) *invariant condition*, for the  $k$ -th ( $k \neq c, k \in \mathcal{C}$ ) disentangled representation,  $E_\phi^k(\hat{x}_0)$  should be the same with  $E_\phi^k(x_0)$ , (ii) *variant condition*, for the  $c$ -th disentangled representation, the conditioned one  $E_\phi^c(\hat{x}_0)$  should be closer to  $E_\phi^c(x_0)$  than the unconditioned one  $E_\phi^c(\hat{x}_0)$ . In the following, we provide the detailed implementation of the above two conditions. According to the above (i) *invariant condition*, the  $k$ -th ( $k \neq c, k \in \mathcal{C}$ ) representation should be kept the same. We encode the two samples using  $E_\phi$  and derive the distance scalar between the  $k$ -th representation as:

$$d_k = \|E_\phi^k(\hat{x}_0^c) - E_\phi^k(x_0)\|. \quad (9)$$

Then the distance vector can be represented as  $d = [d_1, d_2, \dots, d_C]$ . Finally, we use the cross-entropy loss to identify the index  $c$  and restrain others unchanged:

$$\mathcal{L}_{in} = \mathbb{E}_{x_0, t, \epsilon, c} [CrossEntropy(d, c)]. \quad (10)$$

We denote it as invariant loss  $\mathcal{L}_{in}$ .

For the (ii) *variant condition*, we first calculate the distance scalar of the  $k$ -th representation between  $\hat{x}_0$  (unconditioned) and  $x_0, \hat{x}_0^c$  (conditioned) and  $x_0$  as following respectively:

$$\begin{aligned} d_k^n &= \|E_\phi^k(\hat{x}_0) - E_\phi^k(x_0)\| \\ d_k^p &= \|E_\phi^k(\hat{x}_0^c) - E_\phi^k(x_0)\| \end{aligned} \quad (11)$$

According to the above condition (ii), for the conditioned factor  $c$ ,  $d_c^n - d_c^p$  should be maximized, while others, i.e.  $d_k^n - d_k^p$  ( $k \neq c, k \in \mathcal{C}$ ), should be minimized to 0. Similarly we adopt an entropy loss to achieve the subjective as:

$$\mathcal{L}_{va} = \mathbb{E}_{x_0, t, \epsilon, c} [CrossEntropy(d^n - d^p, c)], \quad (12)$$

where  $d^n = [d_1^n, d_2^n, \dots, d_C^n]$  and  $d^p = [d_1^p, d_2^p, \dots, d_C^p]$ . We denote it as variant loss  $\mathcal{L}_{va}$ . So far, we introduce the Disentangling Loss,  $\mathcal{L}_{in}$  and  $\mathcal{L}_{va}$ .

#### 4.4. Total Loss

As we need to satisfy both the *completeness* and *disentanglement* requirements, the total loss includes the above reconstruction loss ( $\mathcal{L}_r$ ) and Disentangling Loss ( $\mathcal{L}_{in}$  and  $\mathcal{L}_{va}$ ). However, the weight to balance the two-part loss should be carefully set. The reason is the following. Note that the above Disentangling Loss  $\mathcal{L}_{in}$  and  $\mathcal{L}_{va}$  is conditioned on the sampled time step of the diffusion process. However, the condition of the diffusion model varies among different time steps. For example, if  $t$  is close to  $T$ ,  $G_\psi^c(x_t, z^c, t)$  mainly condition on  $z^c$ . And if  $t$  is close to 0, the output mainly conditions on  $x_t$ . Therefore, for different time steps, different weights should be used for Disentangling Loss. Considering that the difference between the inputs of encoder reflexes

such change on condition. Specifically, if  $t$  is close to  $T$ , the difference between  $\hat{x}_t$  and  $\hat{x}_t^c$  is small. In addition, if  $t$  is close to 0, such a difference is significant. Based on the above discussion, the more the output condition on  $z^c$ , the higher the weight should be. We thus propose to use the MSE distance between the inputs of the Encoder as the weight coefficient:

$$\gamma_d = \lambda \|\hat{x}_0 - \hat{x}_0^c\|^2, \quad (13)$$

where  $\lambda$  is a hyper-parameter. We stop the gradient of  $\hat{x}_0$  and  $\hat{x}_0^c$  for calculating the weight coefficient  $\gamma_d$ .

The total loss can be calculated as:

$$\mathcal{L}_a = \mathcal{L}_r + \gamma_d(\mathcal{L}_{in} + \mathcal{L}_{va}). \quad (14)$$

#### 4.5. Relation to Total Correlation

In this section, we demonstrate that Total Correlation is a necessary condition for our disentangling loss. Total Correlation is once regarded as an important constraint for representation disentanglement. However, [Locatello et al. \(2019\)](#) point out that besides total Correlation, other inductive biases should also be considered. In this paper, we introduce Disentangling Loss for DPM as an additional inductive bias. We prove that Total Correlation is a necessary condition.

Specifically, if the reconstruction loss is minimized, we have

$$\nabla_{x_t} \log p(z^1, \dots, z^N | x_t) = \sum_{c \in \mathcal{C}} G_\psi^c(x_t, z^c, t) \quad (15)$$

On the other hand, if the disentangling loss is minimized, we have  $G_\psi^c(x_t, z^c, t) = \nabla_{x_t} \log p(z^c | x_t)$ . Since  $\sum_{c \in \mathcal{C}} \nabla_{x_t} \log p(z^c | x_t) = \nabla_{x_t} \log \Pi_{c \in \mathcal{C}} p(z^c | x_t)$  always hold, bring these two equations into Eq. 15, we have

$$\nabla_{x_t} \log p(z^1, \dots, z^N | x_t) = \nabla_{x_t} \log \Pi_{c \in \mathcal{C}} p(z^c | x_t) \quad (16)$$

The equation above results in the fisher divergence between the joint distribution  $p(z^1, \dots, z^N | x_t)$  and the product of marginal distribution  $\Pi_{c \in \mathcal{C}} p(z^c | x_t)$  is 0. Therefore the Total Correlation holds for all  $x_t$ :

$$p(z^1, \dots, z^N | x_t) = \Pi_{c \in \mathcal{C}} p(z^c | x_t) \quad (17)$$

### 5. Experiments

In this section, we conduct experiments to demonstrate the effectiveness of DisDiff on both synthetic and real-world datasets.

#### 5.1. Experimental Setup

**Implementation Details.**  $x_0$  can be an image space or a latent space of images. For image diffusion, we take

Table 1. Comparisons of disentanglement on the FactorVAE score and DCI disentanglement metrics (mean  $\pm$  std, higher is better). DisDiff achieves state-of-the-art performance with a large margin in almost all the cases compared to all baselines. Especially on the MPI3D dataset.

Method	Cars3D		Shapes3D		MPI3D	
	FactorVAE score	DCI	FactorVAE score	DCI	FactorVAE score	DCI
<i>VAE-based:</i>						
FactorVAE	0.906 $\pm$ 0.052	0.161 $\pm$ 0.019	0.840 $\pm$ 0.066	0.611 $\pm$ 0.082	0.152 $\pm$ 0.025	0.240 $\pm$ 0.051
$\beta$ -TCVAE	0.855 $\pm$ 0.082	0.140 $\pm$ 0.019	0.873 $\pm$ 0.074	0.613 $\pm$ 0.114	0.179 $\pm$ 0.017	0.237 $\pm$ 0.056
<i>GAN-based:</i>						
InfoGAN-CR	0.411 $\pm$ 0.013	0.020 $\pm$ 0.011	0.587 $\pm$ 0.058	0.478 $\pm$ 0.055	0.439 $\pm$ 0.061	0.241 $\pm$ 0.075
<i>Pre-trained GAN-based:</i>						
LD	0.852 $\pm$ 0.039	0.216 $\pm$ 0.072	0.805 $\pm$ 0.064	0.380 $\pm$ 0.062	0.391 $\pm$ 0.039	0.196 $\pm$ 0.038
GS	0.932 $\pm$ 0.018	0.209 $\pm$ 0.031	0.788 $\pm$ 0.091	0.284 $\pm$ 0.034	0.465 $\pm$ 0.036	0.229 $\pm$ 0.042
DisCo	0.855 $\pm$ 0.074	0.271 $\pm$ 0.037	0.877 $\pm$ 0.031	0.708 $\pm$ 0.048	0.371 $\pm$ 0.030	0.292 $\pm$ 0.024
<i>Diffusion-based:</i>						
DisDiff-VQ (Ours)	<b>0.976 <math>\pm</math> 0.018</b>	<b>0.232 <math>\pm</math> 0.019</b>	<b>0.902 <math>\pm</math> 0.043</b>	<b>0.723 <math>\pm</math> 0.013</b>	<b>0.617 <math>\pm</math> 0.070</b>	<b>0.337 <math>\pm</math> 0.057</b>

Table 2. Ablation study of DisDiff on image tokenizer, components, batchsize and token numbers.

Method	FactorVAE score	DCI
DisDiff-IM	0.783	0.655
DisDiff-KL	0.837	0.660
DisDiff-VQ	0.902	0.723
DisDiff-VQ wo $\mathcal{L}_{in}$	0.782	0.538
DisDiff-VQ wo $\mathcal{L}_{va}$	0.810	0.620
DisDiff-VQ wo $\mathcal{L}_{dis}$	0.653	0.414
wo detach	0.324	0.026
constant weighting	0.679	0.426
loss weighting	0.678	0.465
attention condition	0.824	0.591
wo pos embedding	0.854	0.678
wo orth embedding	0.807	0.610
latent number $N=6$	0.865	0.654
latent number $N=10$	0.902	0.723

pre-trained DDIM as the DPM (DisDiff-IM). For latent diffusion, we can take the pre-trained KL-version latent diffusion model (LDM) or vq-version LDM as DPM (DisDiff-KL and DisDiff-VQ). For detail of network  $G_\theta$ , we follow Zhang et al. (2022) to use the extended Group Normalization (Dhariwal & Nichol, 2021) by applying scaling & shifting twice. The difference is we use learn-able position

embedding to indicate  $c$ :

$$AdaGN(h, t, z^c) = z_s^c(t_s^c GN(h) + t_b^c) + z_b^c \quad (18)$$

where  $GN$  denotes group normalization, and  $[t_s^c, t_b^c]$ ,  $[z_s^c, z_b^c]$  are obtained from a linear projection:  $z_s^c, z_b^c = linearProj(z^c)$ ,  $t_s^c, t_b^c = linearProj([t, p^c])$ . In addition,  $p^c$  is the learnable positional embedding.  $h$  is the feature map of Unet.

**Datasets** For evaluation of disentanglement, we follow Ren et al. (2021) to use the popular public datasets: Shapes3D (Kim & Mnih, 2018), a dataset of 3D shapes. MPI3D (Gondal et al., 2019), a 3D dataset recorded in a controlled environment, and Cars3D (Reed et al., 2015), a dataset of CAD models generated by color renderings. All experiments are conducted on 64x64 image resolution, which is the same as the literature. For real-world datasets, we conduct our experiments on CelebA (Liu et al., 2015).

**Baselines & Metrics** Since DisDiff is the first diffusion-based disentanglement model. Therefore, we compare the performance with VAE-based and GAN-based baselines. Specifically, the VAE-based models include: FactorVAE (Kim & Mnih, 2018), and  $\beta$ -TCVAE (Chen et al., 2018). The GAN-based baselines include InfoGAN-CR (Lin et al., 2020), GANspace (GS) (Härkönen et al., 2020), LatentDiscovery (LD) (Voynov & Babenko, 2020) and DisCo (Ren et al., 2021). Considering the influence of performance on the random seed. We have 10 runs for each method. We use four representative metrics: FactorVAE score (Kim & Mnih, 2018), and the DCI (Eastwood

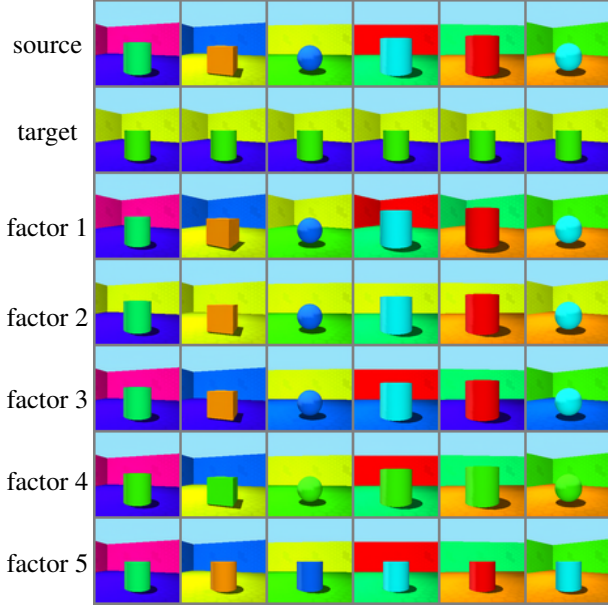


Figure 4. The qualitative results on Shapes3D. The source images provide the representations of the generated image. The target image provides the representations for swapping. Other rows of images are generated by swapping the representation of the corresponding factor on Shapes3D. DisDiff learns pure factors by each representation. The learned factors are azimuth, background color, floor color, object color, and object shape, respectively.

& Williams, 2018). However, since  $\{z^c\}$  are vector-wise representation, we follow Du et al. (2021) to perform PCA as post-processing on the representation before evaluation.

## 5.2. Main Results

We conduct the following experiments to verify the disentanglement ability of proposed DisDiff model. We regard the learned representation  $\{z^c\}$  as the disentangled one and use the popular metrics in disentangled representation literature for evaluation.

The quantitative comparison results of disentanglement under different metrics are shown in Table 1. As shown in the table, DisDiff outperforms the baselines, demonstrating the model’s superior disentanglement ability. Compared with the VAE-based methods, since these methods suffer from the trade-off between generation and disentanglement (Lezama, 2018) but DisDiff does not. As for the GAN-based methods, the disentanglement is learned by exploring the latent space of GAN. Therefore, the performance is limited by the latent space of GAN. DisDiff leverages the gradient field of data space to learn disentanglement and does not have such limitations. In addition, DisDiff resolves the disentanglement problem into 1000 sub-problems under different time steps, which reduces the difficulty.



Figure 5. The qualitative results on CelebA. Each row of images is generated by swapping the representation of the corresponding factor on CelebA. DisDiff learns pure factors by each representation. The learned factors are bangs, skin color, expression, and hair.

## 5.3. Qualitative Results

In order to analyze the disentanglement of DisDiff qualitatively. We swap the representation  $\{z^c\}$  of two images one by one and sample the image conditioned on the swapped representation. We follow LDM-VQ to sample images in 200 steps. For the popular dataset of disentanglement literature, we take shapes3d as an example. As shown in Figure 4, DisDiff successfully learned pure factors. Compared with the VAE-based methods, DisDiff has better image quality. For the real-world dataset, since there are no ground truth factors, we demonstrate the qualitative results in Figure. We take CelebA as an example, as demonstrated in Figure 5, DisDiff also achieves good disentanglement on real-world datasets. Please note that compare with Disco (Ren et al., 2021). DisDiff has the ability of reconstruction, which is not available for DisCo.

## 5.4. Ablation Study

In order to analyze the effectiveness of the proposed parts of DisDiff, we design an ablation study from the following five aspects: DPM type, Disentangling Loss, loss weighting, condition type, and latent number. We take shapes3d as the dataset to conduct these ablation studies.

**DPM type** The disentanglement of DisDiff is derived by the decomposition of the gradient field of the diffusion model. Therefore, the diffusion space influence the performance of DisDiff. We take Shapes3D as an example, it is hard for the model to learn shape and scale in image space, but much easier in the latent space of auto-encoder. Therefore, we compare the performance of DisDiff with different diffusion types: image diffusion model, e.g., DDIM (DisDiff-IM), KL-version latent diffusion model (DisDiff-KL) and VQ-version latent diffusion model, e.g., VQ-LDM (DisDiff-VQ).



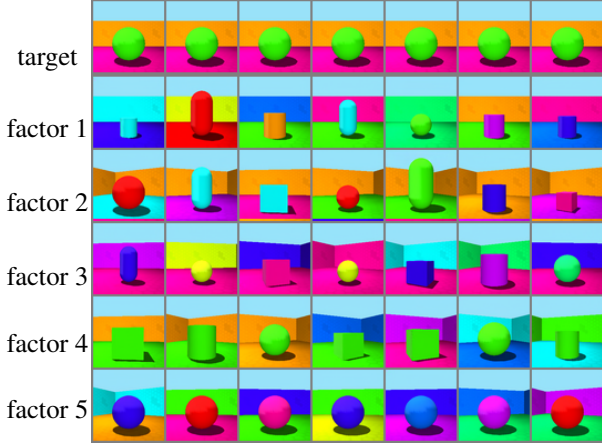


Figure 6. The partially condition sampling on Shapes3D. The target image provides the representation of partially sampling image. Each row of images are generated by imposing a single gradient field of the corresponding factor on the pre-trained DPM. DisDiff samples image condition on only a single factor. The sampled image has a fixed factor, e.g., the images of factor 1 have same background color with target one. The conditioned factors are: azimuth, background color, floor color, object color and object shape, respectively.

As shown in Table 2, the LDM-version DisDiff outperforms image-version DisDiff as expected. In addition, KL-LDM has more complex latent space than VQ-LDM. DisDiff-VQ outperforms DisDiff-KL.

**Disentangling Loss** Disentangling loss is composed of two parts: Invariant loss  $\mathcal{L}_{in}$  and Variant loss  $\mathcal{L}_{va}$ . In order to verify the effectiveness of each part, we train DisDiff-VQ without it.  $\mathcal{L}_{in}$  encourages in-variance of representation not being sampled, which means that the sampled factor will not affect the representation of other factors ( $z^k, k \neq l$  of generated  $\hat{x}_0^l$ ). On the other hand,  $\mathcal{L}_{va}$  encourages the representation of sampled factor ( $z^l$  of generated  $\hat{x}_0^l$ ) should be close to the corresponding one of  $x_0$ . As shown in Table 2, mainly  $\mathcal{L}_{in}$  encourage the disentanglement, and  $\mathcal{L}_{va}$  further constrain the model and improve the performance. Note that the disentangling loss is optimized w.r.t.  $G_\theta$  but not  $E_\theta^c$ . If the loss is optimized on both modules, as shown in Table 2, DisDiff fails to achieve disentanglement. The reason is that the disentangling loss influenced the encoder, so DisDiff failed to reconstruct the input image.

**Loss weighting** As introduced, considering that the condition varies among time steps, we adopt the difference of the encoder as the weight coefficient. In this section, we explore other options to verify its effectiveness. We offer two different weighting types: constant weighting and loss weighting. The first type is the transitional way of weighting. The second one is to balance the scale of Disentangling Loss and diffusion loss. From Table 2, these two types of weighting hurt the performance to a different extent.



Figure 7. The partially condition sampling on CelebA. The target image provides the representations of the sampling image. Images of each row are conditioned on a single factor. DisDiff samples image condition on only a single factor. Therefore, the sampled image in the same row has a fixed factor, e.g., the images of factor 1 have the same background as the target one. The conditioned factors are background, skin color, expression, and hair, respectively.

**Condition type** DisDiff follows PADE (Zhang et al., 2022) and (Dhariwal & Nichol, 2021) to adopt AdaGN for injecting the condition. However, there is another option in the literature: cross-attention. As shown in Table 2, cross-attention hurt the performance but not much. We infer that the reason may be that the condition is only a single token, which limits the ability of attention. We use learnable orthogonal positional embedding to indicate different factors. As shown in Table 2, no matter whether no positional embedding (wo pos embedding) or traditional learnable positional embedding (wo orth embedding) hurt the performance. The reason is that the orthogonal embedding is always different from each other in all training steps.

**Latent number** The number of latent is a important hyper-parameter set in-advance. We conduct ablation study on this hyper-parameter. As shown in Table 2, the latent number only has limited influence on the performance.

### 5.5. Partially Condition Sampling

As discussed in Section 4.2, DisDiff can partially sample conditions on the part of the factors. Specifically, we can use Equation 6 to sample image condition on factors set  $\mathcal{S}$ . We take Shapes3D, as an example, when DisDiff sampling image condition on background color is red. We obtain a set of images of the background color red and other factors randomly sampled. From Figure 6, we see that DisDiff has the ability to condition individual factors on Shapes3D. In addition, DisDiff also has such ability on the real-world dataset (CelebA) in Figure 7. DisDiff has the ability to sample information exclusively to conditions.

## 6. Conclusion

In this paper, we demonstrate a new task: disentanglement of DPM, by disentangling a DPM into several disentangled



gradient fields, we can improve the interpretability of DPM. To solve the task, we build an unsupervised diffusion-based disentanglement framework named DisDiff. DisDiff learns a disentangled representation of the input image in the diffusion process. In addition, for each factor, DisDiff learns a disentangled gradient field, which brings the following new properties for disentanglement literature. DisDiff adopted disentangling constraints on all different timesteps, which is a new inductive bias. Except for image editing, with the disentangled DPM, we also can sample partially conditions on the part of the information by superposition of the sub-gradient field. For future work, Applying DisDiff to more general conditioned DPM is a direction worth exploring. Besides, utilizing the proposed disentangling method to pre-trained conditional DPM makes it more flexible.

## References

- Avrahami, O., Lischinski, D., and Fried, O. Blended diffusion for text-driven editing of natural images. In *Proceedings of the IEEE/CVF Conference on Computer Vision and Pattern Recognition*, pp. 18208–18218, 2022.
- Bengio, Y., Courville, A. C., and Vincent, P. Representation learning: A review and new perspectives. *PAMI*, 2013.
- Burgess, C. P., Higgins, I., Pal, A., Matthey, L., Watters, N., Desjardins, G., and Lerchner, A. Understanding disentanglement in beta-vae. *arXiv:1804.03599*, 2018.
- Chen, R. T., Li, X., Grosse, R. B., and Duvenaud, D. K. Isolating sources of disentanglement in variational autoencoders. In *NeurIPS*, 2018.
- Choi, J., Kim, S., Jeong, Y., Gwon, Y., and Yoon, S. Ilvr: Conditioning method for denoising diffusion probabilistic models. *arXiv preprint arXiv:2108.02938*, 2021.
- Dhariwal, P. and Nichol, A. Diffusion models beat gans on image synthesis. *Advances in Neural Information Processing Systems*, 34:8780–8794, 2021.
- Du, Y., Li, S., Sharma, Y., Tenenbaum, J., and Mordatch, I. Unsupervised learning of compositional energy concepts. *Advances in Neural Information Processing Systems*, 34, 2021.
- Eastwood, C. and Williams, C. K. I. A framework for the quantitative evaluation of disentangled representations. In *ICLR*, 2018.
- Gondal, M. W., Wuthrich, M., Miladinovic, D., Locatello, F., Breidt, M., Volchkov, V., Akpo, J., Bachem, O., Schölkopf, B., and Bauer, S. On the transfer of inductive bias from simulation to the real world: a new disentanglement dataset. In *NeurIPS*, 2019.
- Goodfellow, I., Pouget-Abadie, J., Mirza, M., Xu, B., Warde-Farley, D., Ozair, S., Courville, A., and Bengio, Y. Generative adversarial networks. *Communications of the ACM*, 63(11):139–144, 2020.
- Härkönen, E., Hertzmann, A., Lehtinen, J., and Paris, S. Ganspace: Discovering interpretable GAN controls. In *NeurIPS*, 2020.
- Higgins, I., Matthey, L., Pal, A., Burgess, C., Glorot, X., Botvinick, M., Mohamed, S., and Lerchner, A. beta-vae: Learning basic visual concepts with a constrained variational framework. In *ICLR*, 2017.
- Higgins, I., Amos, D., Pfau, D., Racaniere, S., Matthey, L., Rezende, D., and Lerchner, A. Towards a definition of disentangled representations. *arXiv preprint arXiv:1812.02230*, 2018.
- Ho, J. and Salimans, T. Classifier-free diffusion guidance. *arXiv preprint arXiv:2207.12598*, 2022.
- Ho, J., Jain, A., and Abbeel, P. Denoising diffusion probabilistic models. *Advances in Neural Information Processing Systems*, 33:6840–6851, 2020.
- Jolicoeur-Martineau, A., Piché-Taillefer, R., Combes, R. T. d., and Mitliagkas, I. Adversarial score matching and improved sampling for image generation. *arXiv preprint arXiv:2009.05475*, 2020.
- Kawar, B., Zada, S., Lang, O., Tov, O., Chang, H., Dekel, T., Mosseri, I., and Irani, M. Imagic: Text-based real image editing with diffusion models. *arXiv preprint arXiv:2210.09276*, 2022.
- Kim, G., Kwon, T., and Ye, J. C. Diffusionclip: Text-guided diffusion models for robust image manipulation. In *Proceedings of the IEEE/CVF Conference on Computer Vision and Pattern Recognition*, pp. 2426–2435, 2022.
- Kim, H. and Mnih, A. Disentangling by factorising. In *ICML*, 2018.
- Kwon, M., Jeong, J., and Uh, Y. Diffusion models already have a semantic latent space. *arXiv preprint arXiv:2210.10960*, 2022.
- Lezama, J. Overcoming the disentanglement vs reconstruction trade-off via jacobian supervision. In *International Conference on Learning Representations*, 2018.
- Lin, Z., Thekumparampil, K., Fanti, G., and Oh, S. Infogan-cr and modelcentrality: Self-supervised model training and selection for disentangling gans. In *ICML*, 2020.

- Liu, X., Park, D. H., Azadi, S., Zhang, G., Chopikyan, A., Hu, Y., Shi, H., Rohrbach, A., and Darrell, T. More control for free! image synthesis with semantic diffusion guidance. In *Proceedings of the IEEE/CVF Winter Conference on Applications of Computer Vision*, pp. 289–299, 2023.
- Liu, Z., Luo, P., Wang, X., and Tang, X. Deep learning face attributes in the wild. In *Proceedings of International Conference on Computer Vision (ICCV)*, December 2015.
- Locatello, F., Bauer, S., Lucic, M., Raetsch, G., Gelly, S., Schölkopf, B., and Bachem, O. Challenging common assumptions in the unsupervised learning of disentangled representations. In *international conference on machine learning*, pp. 4114–4124. PMLR, 2019.
- Lugmayr, A., Danelljan, M., Romero, A., Yu, F., Timofte, R., and Van Gool, L. Repaint: Inpainting using denoising diffusion probabilistic models. In *Proceedings of the IEEE/CVF Conference on Computer Vision and Pattern Recognition*, pp. 11461–11471, 2022.
- Meng, C., He, Y., Song, Y., Song, J., Wu, J., Zhu, J.-Y., and Ermon, S. Sedit: Guided image synthesis and editing with stochastic differential equations. In *International Conference on Learning Representations*, 2021.
- Preechakul, K., Chatthee, N., Wizadwongsa, S., and Suwajanakorn, S. Diffusion autoencoders: Toward a meaningful and decodable representation. In *IEEE Conference on Computer Vision and Pattern Recognition (CVPR)*, 2022.
- Radford, A., Kim, J. W., Hallacy, C., Ramesh, A., Goh, G., Agarwal, S., Sastry, G., Askell, A., Mishkin, P., Clark, J., et al. Learning transferable visual models from natural language supervision. In *International Conference on Machine Learning*, pp. 8748–8763. PMLR, 2021.
- Reed, S. E., Zhang, Y., Zhang, Y., and Lee, H. Deep visual analogy-making. In *NeurIPS*, 2015.
- Ren, X., Yang, T., Wang, Y., and Zeng, W. Learning disentangled representation by exploiting pretrained generative models: A contrastive learning view. In *International Conference on Learning Representations*, 2021.
- Saharia, C., Chan, W., Saxena, S., Li, L., Whang, J., Denton, E., Ghasemipour, S. K. S., Ayan, B. K., Mahdavi, S. S., Lopes, R. G., et al. Photorealistic text-to-image diffusion models with deep language understanding. *arXiv preprint arXiv:2205.11487*, 2022.
- Sohl-Dickstein, J., Weiss, E., Maheswaranathan, N., and Ganguli, S. Deep unsupervised learning using nonequilibrium thermodynamics. In *International Conference on Machine Learning*, pp. 2256–2265. PMLR, 2015.
- Song, J., Meng, C., and Ermon, S. Denoising diffusion implicit models. *arXiv preprint arXiv:2010.02502*, 2020a.
- Song, Y. and Ermon, S. Generative modeling by estimating gradients of the data distribution. *Advances in Neural Information Processing Systems*, 32, 2019.
- Song, Y., Sohl-Dickstein, J., Kingma, D. P., Kumar, A., Ermon, S., and Poole, B. Score-based generative modeling through stochastic differential equations. *ICLR*, 2020b.
- Srivastava, A., Bansal, Y., Ding, Y., Hurwitz, C. L., Xu, K., Egger, B., Sattigeri, P., Tenenbaum, J., Cox, D. D., and Gutfreund, D. Improving the reconstruction of disentangled representation learners via multi-stage modelling. *CoRR*, abs/2010.13187, 2020.
- Voynov, A. and Babenko, A. Unsupervised discovery of interpretable directions in the GAN latent space. In *ICML*, 2020.
- Wang, T., Zhang, Y., Fan, Y., Wang, J., and Chen, Q. High-fidelity gan inversion for image attribute editing. In *Proceedings of the IEEE/CVF Conference on Computer Vision and Pattern Recognition*, pp. 11379–11388, 2022.
- Yang, T., Ren, X., Wang, Y., Zeng, W., and Zheng, N. Towards building a group-based unsupervised representation disentanglement framework. In *International Conference on Learning Representations*, 2021.
- Zhang, Z., Zhao, Z., and Lin, Z. Unsupervised representation learning from pre-trained diffusion probabilistic models. *NeurIPS*, 2022.